An Improvement for Tomographic Density Imaging using Integration of DBIM and Interpolation

Nguyen Thi Hoang Yen
Hanoi National University of Education,
Hanoi, Vietnam
hoangyenspkt@gmail.com

Ngo Van Cong
Vietnam Metrology Institute
Hanoi, Vietnam
congnv@vmi.gov.vn

Phung Cong Phi Khanh
Hanoi National University of Education,
Hanoi, Vietnam
phungcongphikhanh@gmail.com

Nguyen Ha Huy Cuong
Quangnam University
Quangnam, Vietnam
nguyenhahuycuong@gmail.com

Vijender Kumar Solanki
CMR Institute of Technology Hyderabad
TS, India
spesinfo@yahoo.com

Duc-Tan Tran
University of Engineering and Technology
Hanoi, Vietnam
tantd@vnu.edu.vn

Abstract— **Inverse scattering is considered to be one of the most powerful and accurate ultrasound imaging. Most ultrasound tomography methods often focus to the speed of sound and ignore the change of density in tomographic imaging. Convergence speed of density imaging is also higher than that of sound contrast imaging. Thus, in this paper, we proposed to speed up the reconstructed time of tomographic density imaging by integrating the distorted Born iterative method (DBIM) and interpolation scheme. The result is improved both the reconstructed quality and the reconstructed time.**

Keywords—density, tomography, DBIM

I. INTRODUCTION

Ultrasound imaging is now widely used for medical applications [1]. In current ultrasound machines, however, it is difficult to reconstruct structures smaller than the wavelength. Tomographic ultrasound exploits the inverse scattering technique can do this [2]. We can recognize strange tumors because when the ultrasound signal passes through it, the sound contrast will change. Distorted Born Iterative Method (DBIM) method is preferred in tomographic ultrasound because it allows the linear relationship between the ultrasound signal to be measured with the sound contrast when ultrasound passes through the tumor [3-7]. Most of previous work only focusses to sound contrast imaging [3-7, 11-16]. In [8], DBIM is also applied to tomographic density imaging, and obtain very nice results. However, the authors need to collect multiple datasets at multiple frequencies that lead to increase the acquisition time. In [11-12], the authors concerned to apply deterministic compressive sampling (CS) for high-quality image reconstruction of ultrasound tomography. However, the reconstruction time in CS scheme is always large. In this paper, we integrate DBIM with interpolation technique in order to improve both the reconstructed quality and the reconstructed time. The reconstruction is divided into two steps. In the first step, DBIM is applied to estimate the object function with a low mesh. The interpolation is then applied to acquire a new object function with a dense mesh. In the second step, DBIM continue to work with this new object function to provide a final tomographic density image.

II. METHOD PROPOSAL

A. Object function for density imaging

A measurement system is shown in Fig. 1 in order to acquire the scattered signal. As can we see, one transmitter and one receiver are executed to obtain a measured signal. After that, DBIM is used to reconstruct the object function for density imaging.

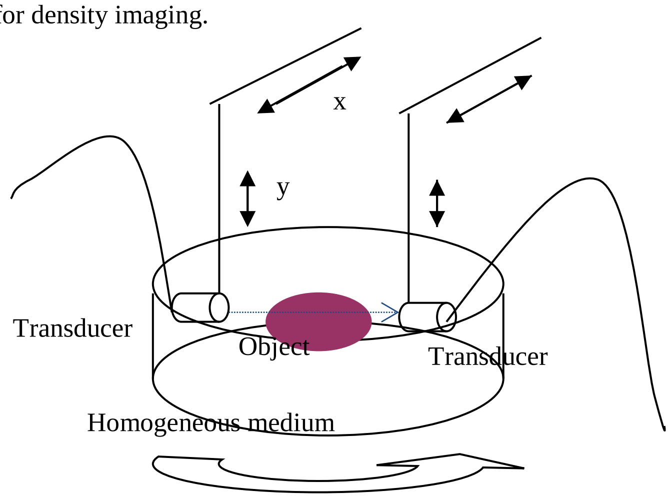

Fig 1. Measurement system

In detail, the wave equation of the measurement system is

$$p(\vec{r}) = p^{inc}(\vec{r}) + p^{sc}(\vec{r}) \quad (1)$$

where $p(\vec{r})$, $p^{inc}(\vec{r})$, and $p^{sc}(\vec{r})$ are the total pressure, incident pressure and scattered pressure fields, respectively. $p^{sc}(\vec{r})$ can be shown in more detail as

$$p^{sc}(\vec{r}) = \iint O(\vec{r'})\, p(\vec{r'})\, G_0(|\vec{r} - \vec{r'}|)\, d\vec{r'} \quad (2)$$

where $G_0(.)$ is the homogenous Green function, and $O(\vec{r})$ is the object function need to be reconstructed. If there is an object whose a constant density and a wave number *k(r)* in this medium, the object function $O(\vec{r})$ is

$$O(\vec{r}) = \left(\left(\frac{\omega}{c(\vec{r})}\right)^2 - \left(\frac{\omega}{c_0}\right)^2\right) \quad (3)$$

978-1-5386-2599-6/18/$31.00 ©2018 IEEE

where c_0 is the sound speed in the infinite space containing homogeneous medium, and *c(r)* is the sound speed travels through the object. In this paper, we also concern the role of the density, thus the object function $O(\vec{r})$ is

$$\mathcal{O}\ (\vec{r}) = \left(\left(\frac{\omega}{c(\vec{r})}\right)^2 - \left(\frac{\omega}{c_0}\right)^2\right) - \rho^{1/2}(\vec{r})\nabla^2\rho^{-1/2}(\vec{r}) \quad (4)$$

Figure 2(a)(b) illustrates the differences between sound contrast imaging and density imaging. The ripples appear on the border of the object and the medium. We also can see that the reconstruction of the object function for density imaging is more difficult than one of sound contrast imaging. The scattered data is processed using DBIM as shown in the literature [9, 13-16].

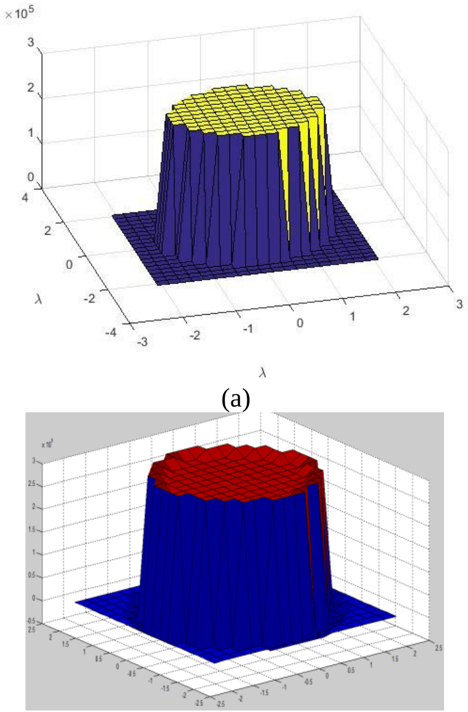

(a)

(b)

Fig 2. The difference between the object function for density imaging and sound contrast imaging.

B. Density imaging using integration of DBIM and interpolation

The proposed method consists of three steps. In the first step, the object function is reconstructed with the resolution of $N_1 \times N_1$. The convergence is expected to approach because N_1 is small enough. In the second step, the object function with low resolution is put into the interpolation to obtain a new object function with the size of $N_2 \times N_2$. In the last step, this new object function is continued with DBIM to complete the reconstruction. The interpolation used in this paper is nearest neighbor because it is simple and fast [10]. In this paper, we propose a flow chart to summarize the reconstructed process:

Algorithm 1. Density imaging using DBIM and Interpolation

1: Choose an initial value of $\overline{O}_{N_1}{}^{(0)}$ and $\overline{p}^{(0)} = \overline{p}_{N_1}{}^{inc}$

2: While (n < N_{max1}) or ($RRE_{N1} < \varepsilon_{N_1}$) do

{

3: Compute two matrices $\overline{B}_{N_1}$ and $\overline{C}_{N_1}$; $\overline{p}$ and p^{sc} correspond to $\overline{O}_{N_1}{}^{(n)}$.

4: Compute the vector $\Delta\overline{p}^{sc}$

5: Compute RRE correspond to $\overline{\Delta O}_{N_1}{}^{(n)}$

6: Compute a new $\overline{O}_{N_1}{}^{(n+1)}$

7: n=n+1; }

8: Interpolate $\overline{O}_{N_1}{}^{(n)}$ to obtain $\overline{O}_{N_2}{}^{(0)}$

9: Set $\overline{p}^{(0)} = \overline{p}_{N_2}{}^{inc}$, n=0

10: While (n < N_{max2}) or ($RRE_{N2} < \varepsilon_{N_2}$) do

{

11: Compute two matrices $\overline{B}_{N_2}$ and $\overline{C}_{N_2}$; $\overline{p}$ and p^{sc} correspond to $\overline{O}_{N_2}{}^{(n)}$ using equation (3) and (4).

12: Compute the vector $\Delta\overline{p}^{sc}$

13: Compute RRE correspond to $\overline{\Delta O}_{N_2}{}^{(n)}$

14: Compute a new $\overline{O}_{N_2}{}^{(n+1)}$

15: n=n+1;

}

where N_{max1} and N_{max2} are the maximum numbers of iterations, ε_{N_1} and ε_{N_2} are stopping errors determined by noise floor, RRE_{N1} and RRE_{N2} are relative residual errors. The definition of RRE is

$$RRE = \sum_{i=1}^{N}\sum_{j=1}^{N}\frac{|o_{ij} - \hat{o}_{ij}|}{o_{ij}} \quad (5)$$

III. RESULTS AND DISCUSSIONS

In order to verify our proposed method, a simulation scenario is established as shown in Table 1.

TABLE 1. Simulation scenario

Frequency of ultrasound signal	0.64MHz
Diamter of scatter area	1mm
Number of pixels	N_1 = 14; N_2 = 27
Number of transmitters N_t	21
Number of receivers N_r	11
Speed of sound contrast Δc	2%
N_{max}	8

Figures 3-10 show the comparison between our proposed and conventional DBIM methods in 8 iterations. Figs. 3-10(b) shows the reconstructed results of the object function using conventional DBIM with the resolution of 27 × 27. After eight iterations, the object function is reconstructed with a lower quality. For our proposed methods, Figs. 3-6(a) show the object function is well reconstructed a low resolution 14 × 14 after 4 iterations (N_{max1}=4). The convergence is achieved easily with this resolution. After that, the object function with low resolution 14 × 14 is put into the interpolation to obtain a new object function with the size of 27 × 27. Figs. 7-10(a) show the object function is well reconstructed a higher resolution 27 × 27.

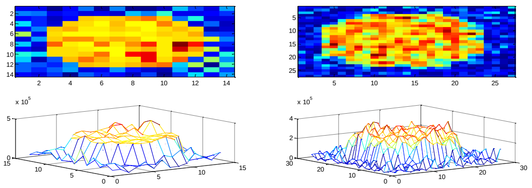

a) 14 × 14 – proposed b) 27 × 27 – conventional

Fig. 3. Reconstruction of the object function after the first iteration (N_1 = 14, N_2 = 27)

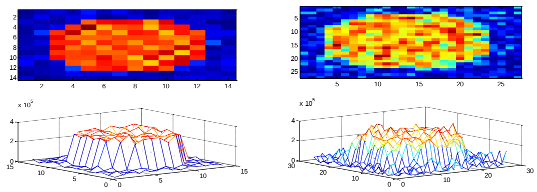

a) 14 ×14 – proposed b) 27 × 27 – conventional

Fig. 4. Reconstruction of the object function after two iterations (N_1 = 14, N_2 = 27)

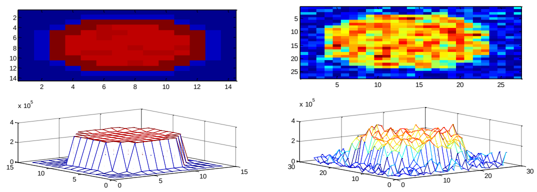

a) 14 × 14 – proposed b) 27 × 27 – conventional

Fig. 5. Reconstruction of the object function after three iterations (N_1 = 14, N_2 = 27)

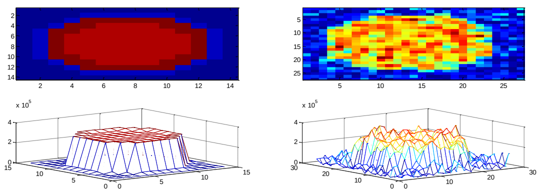

a) 14 × 14 – proposed b) 27 × 27 – conventional

Fig. 6. Reconstruction of the object function after four iterations (N_1 = 14, N_2 = 27)

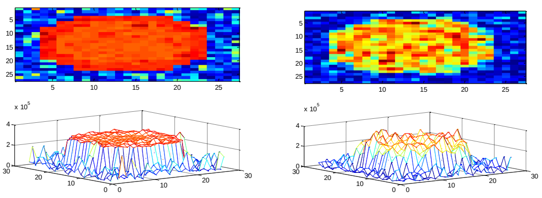

a) 27 × 27 – proposed b) 27×27 – conventional

Fig. 7. Reconstruction of the object function after five iterations

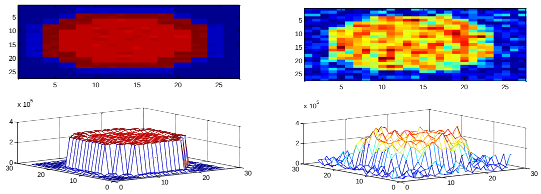

a) 27 × 27 – proposed b) 27 × 27 – conventional

Fig. 8. Reconstruction of the object function after six iterations

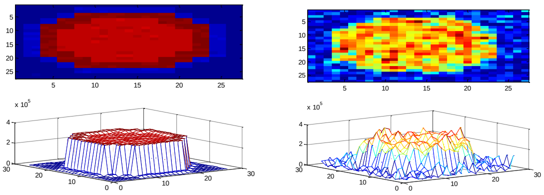

a) 27 × 27 – proposed b) 27 × 27 – conventional

Fig. 9. Reconstruction of the object function after seven iterations

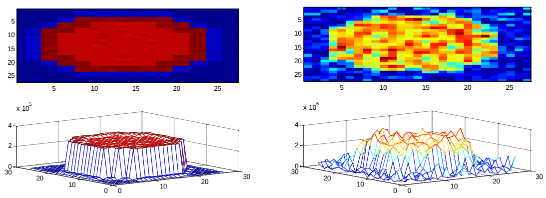

a) 27 × 27 – proposed b) 27 × 27 – conventional

Fig. 10. Reconstruction of the object function after eight iterations

Comparisons:

- *Error in reconstruction:* It can be seen that our proposed method offer a better reconstruction quality compared to conventional one (see Fig. 10); thus, provide a smaller error.
- *Reconstruction time:* Both methods need 8 iterations, but our proposed methods offer a lower reconstruction time because from the 1^{st} to 4^{th} iteration, it works with a low resolution.

IV. CONCLUSION

In this paper, we applied DBIM and interpolation technique in order to speed up the density imaging. A simulation scenario has been used to prove the effectiveness of our proposed method. The results that we can both improve the reconstruction time and reconstructed quality. Interpolation technique is helpful to support the convergence of other tomographic density imaging algorithms. Our method can be further developed by 3D reconstruction and experiment.

REFERENCES

[1] C.F. Schueler, H.Lee, and G. Wade,"Fundamentals of digital ultrasonic processing," IEEETransactionsonSonicsandUltrasonics,vol.31,no.4, pp.195–217, July 1984.

[2] Lavarello Robert: New Developments on Quantitative Imaging Using Ultrasonic Waves. University of Illinois at Urbana-Champaign, 2009.

[3] Devaney AJ (1982) Inversion formula for inverse scattering within the Born approximation. Optics Letters 7:111-112.

[4] Lujiang Liu, Xiaodong Zhang, and Shira L. Broschat, "Ultrasound Imaging Using Variations of the Iterative Born Technique", IEEE

transactions on ultrasonics, ferroelectrics, and frequency control, vol. 46, no. 3, May 1999.

[5] Jonathan Mamou, Michael L.Oelze, “Quantitative Ultrasound in Soft Tissues”, DOI:10.1007/978-94-007-6952-6_2, Springer Science + Business Media Dordrecht 2013.

[6] Haddadin OS, Ebbini ES (1995) Solution to the inverse scattering problem using a modified distorted Born iterative algorithm. Proceedings of IEEE Ultrasonics Symposium, 1411-1414.

[7] Hesford AJ, Chew WC (2010) Fast inverse scattering solutions using the distorted Born iterative method and the multilevel fast multipole algorithm. J Acous Soc America, 128:679-690.

[8] Lavarello R, Oelze M, Density imaging using a multiple-frequency DBIM approach, IEEE Trans UltrasonFerroelectrFreq Control. 2010 Nov; 57(11):2471-9. doi: 10.1109/TUFFC.2010.1713.

[9] Gene H. Golub, Per Christian Hansen, and Dianne P. O’Leary: Tikhonov Regularization and Total Least Squares. SIAM Journal on Matrix Analysis and Applications. Vol. 21 Issue 1, Aug. 1999.

[10] Jegou, H., Douze, M., & Schmid, C. (2011). Product quantization for nearest neighbor search. Pattern Analysis and Machine Intelligence, IEEE Transactions on, 33(1), 117-128.

[11] Huy, T. Q., Tue, H. H., Long, T. T., & Duc-Tan, T. (2017). Deterministic compressive sampling for high-quality image reconstruction of ultrasound tomography. BMC medical imaging, 17(1), 34.

[12] Quang-Huy, T., & Duc-Tan, T. (2016, October). Integration of compressed sensing and frequency hopping techniques for ultrasound tomography. In Advanced Technologies for Communications (ATC), 2016 International Conference on (pp. 442-446). IEEE.

[13] Tran, Q. H., Tran, D. T., Huynh, H. T., Ton-That, L., & Nguyen, L. T. (2016). Influence of dual-frequency combination on the quality improvement of ultrasound tomography. Simulation, 92(3), 267-276.

[14] Quang-Huy, T., & Duc-Tan, T. (2015, October). Sound contrast imaging using uniform ring configuration of transducers with reconstruction. In Advanced Technologies for Communications (ATC), 2015 International Conference on (pp. 149-153). IEEE.

[15] Tran, Q. H., & Tran, D. T. (2015). Ultrasound Tomography in Circular Measurement Configuration using Nonlinear Reconstruction Method. International Journal of Engineering and Technology (IJET), 7(6), 2207-2217.

[16] Tran-Duc, T., Linh-Trung, N., Oelze, M. L., & Do, M. N. (2013). Application of l_1 Regularization for High-Quality Reconstruction of Ultrasound Tomography. In 4th International Conference on Biomedical Engineering in Vietnam (pp. 309-312). Springer, Berlin, Heidelberg.